water

MDPI

Article

Heavy Rainfall Triggering Shallow Landslides: A Susceptibility Assessment by a GIS-Approach in a Ligurian Apennine Catchment (Italy)

Anna Roccati [1], Francesco Faccini [1,2,*], Fabio Luino [1], Andrea Ciampalini [3] and Laura Turconi [1]

1 Istituto di Ricerca per la Protezione Idrogeologica, Consiglio Nazionale delle Ricerche, Strada delle Cacce 73, 10135 Torino, Italy; anna.roccati@fastwebnet.it (A.R.); fabio.luino@irpi.cnr.it (F.L.); laura.turconi@irpi.cnr.it (L.T.)

2 Dipartimento di Scienze della Terra, dell'Ambiente e della Vita, Università di Genova, corso Europa 26, 16132 Genova, Italy

3 Dipartimento di Scienze della Terra, Università di Pisa, via S. Maria 53, 56126 Pisa, Italy; andrea.ciampalini@unipi.it

* Correspondence: faccini@unige.it; Tel.: +39-0103538039

Received: 18 February 2019; Accepted: 20 March 2019; Published: 23 March 2019

Abstract: In recent decades, the Entella River basin (eastern Liguria) has been affected by several rainfall events that induced widespread shallow landslides and earth flows on the slopes; roads, buildings, structures and infrastructure suffered extensive damage due to the instability processes. In this paper, a GIS-based approach for analyzing and assessing a simplified landslide susceptibility in the Entella River catchment is presented. Starting from landslide information mainly provided from newspaper articles and unpublished reports from municipal archives, we performed a series of comparative analyses using a set of thematic maps to assess the influence of predisposing natural and anthropic factors. By evaluating the statistical distribution of landslides in different categories, we assigned weighted values to each parameter, according to their influence on the instability processes. A simplified, reproducible, but effective approach to assess landslide susceptibility in the study area was performed by combining all predisposing factors. The resulting scores in proneness to slope instability classes may be used to generate a simplified landslides susceptibility map of the catchment area which would be easy to regularly update every time a rainfall event that is able to trigger shallow landslides occurs; this would provide a useful tool for local authorities and decision makers for identifying areas which could potentially be affected by instability processes, and would help in determining the most suitable measures in land-planning and landslide risk management.

Keywords: shallow landslides; heavy rainfall; anthropic disturbance; susceptibility; GIS

1. Introduction

In the last 50 years, thousands of shallow landslides induced by heavy rainfall events have affected hilly and mountainous regions throughout the world [1–5]. Destructive slope mass-movements, due to very short but heavy or intense prolonged rainfall, kill people every year and cause countless socio-economic damage. In modern urban society, a large portion of the population is exposed to landslides risk, which is greatly increased by global climate change [6,7], human interventions and landscape modifications, i.e., urbanization, deforestation, land-changes and the abandonment of rural areas [8–13]. Rainfall-induced shallow landslides initiate mainly on steep and very steep slopes, and involve small thickness materials originating from the weathering of the bedrock, as well as from soil erosion and downslope transportation due to meteoric and running waters. Occasionally, slope

failure involves a portion of the fractured and weathered bedrock. Despite the small soil volumes involved, shallow landslides frequently cause extensive damage to man-made structures, and can be particularly destructive when channeled, thereby evolving into debris flows [14–17]. With a high velocity of propagation, especially when sliding materials flow like a fluid, the presence of boulders in the flow and widespread spatial distribution across territories contribute to increasing their destructive power [18].

Our understanding of the triggering mechanisms of rainfall-induced shallow landslides, and the prediction of their occurrence, have been two of the most studied topics in recent decades. In the literature, different approaches have been proposed to evaluate the interactions between shallow landslides and the role of the numerous geological, geomorphological, environmental and human-influenced predisposing factors involved in slope failures. Using slope stability calculation, various physically-based models have been developed [19–24]. However, these approaches are complicated to apply because of the numerous variables involved in triggering shallow landslides (e.g., slope morphology, vegetation coverage, lithology, hydraulic soil properties, thickness of the debris cover, rainfall variations, land-use, etc.), which are difficult to estimate accurately, and can vary in space and time, particularly over large regions. Many studies on landslide susceptibility assessment have been performed to evaluate potential slope instability; from this perspective, landslide susceptibility maps can be used as operative tools in land-planning for landslide hazard and risk management, and for the implementation of early warning systems [25]. Several methods and techniques have been proposed to evaluate susceptibility to landslides [26–29] based on different qualitative and quantitative approaches and geo-environmental information, e.g., landslide inventory maps, predisposing and triggering factors, etc. [30,31], often using geographical information systems (GISs) [32–35]. Among data-driven landslide susceptibility assessments, in the literature, different methodologies have been performed based on statistical [36–40], probabilistic [41–44] and machine-learning [45–47] approaches or physical-based methods [48,49].

The Liguria region, northern Italy, is a Mediterranean area in which landslide hazards are very high, due to the region's geological and morphological setting and particular climatic conditions. In recent decades, Liguria has suffered several rainfall events that resulted in widespread ground effects on the slopes, with extensive damage to private and public property, infrastructure and businesses, as well as a number of casualties [50–58]. Shallow landslides and earth flows occur mainly in areas which have been significantly modified by human activity, through agricultural (or farming) terraces, road networks, river modifications (including narrowing, channelization, and partial or complete coverage) and artificial surfaces [59–63].

In this paper, a GIS-based approach for analyzing and assessing landslide susceptibility in the Entella river catchment is presented. First, we discuss the ground effects induced on the slopes by heavy rainfall events in the study area over the period 2000–2017; in the 17-year interval, the basin suffered a total of 45 damaging rainfall events (2.6 per year on average, with a maximum of 8 events in 2013 and 2014), which caused hundreds of shallow landslides and earth flows along the slopes, and two fatalities [56,64–66]. A landslide inventory was added to a GIS platform and correlated with a set of thematic maps to evaluate the roles of different controlling factors in predisposing slope gravitational processes (e.g., lithology, slope acclivity and aspect, land-use, drainage patterns and anthropic structures) and the influence of human disturbance on slope stability. By evaluating the spatial distribution of landslides of different classes, we assigned weighted values to each parameter and, finally, combined this information to assess scores assigned to susceptibility classes, that may be used to generate a landslide susceptibility map of the catchment area and to provide a useful tool for local authorities in land-planning and landslide risk management.

Almost all existing studies comprising conventional landslide susceptibility assessments use different approaches comprising several sets of structured and homogeneous data, mainly based on landslide inventory databases and archives which are usually compiled using field surveys or remote sensing, and which are not continually updated [67]. Moreover, they generally do not include

analyses of human impact as a factor which can contribute to shallow landslides. The main innovative contribution of this work is to perform analyses using unstructured and heterogeneous landslide information, which will be easy to find and fairly regularly-updated (mainly from newspapers articles, chronicle notes from local and social media, interviews with local inhabitants and damage reports compiled by local authorities), and which will include anthropogenic elements (e.g., roads, buildings, man-made structures) among predisposing factors, in addition to the development of a simplified, reproducible but effective approach to assessing landslide prone areas that can be easily applied in different hilly and mountain catchment areas affected by rainfall-induced shallow landslides.

2. Materials and Methods

2.1. Study Area

The study area corresponds to the Entella River basin, one of the main Ligurian catchment areas (Figure 1). It extends for 370 km^2 and is formed by the Lavagna (160 km^2), Sturla (130 km^2) and Graveglia (63 km^2) tributaries. The Entella River rises with the confluence of the Lavagna and Graveglia Streams, and 4 km downstream, with the contribution of the third watercourse, the Sturla Stream.

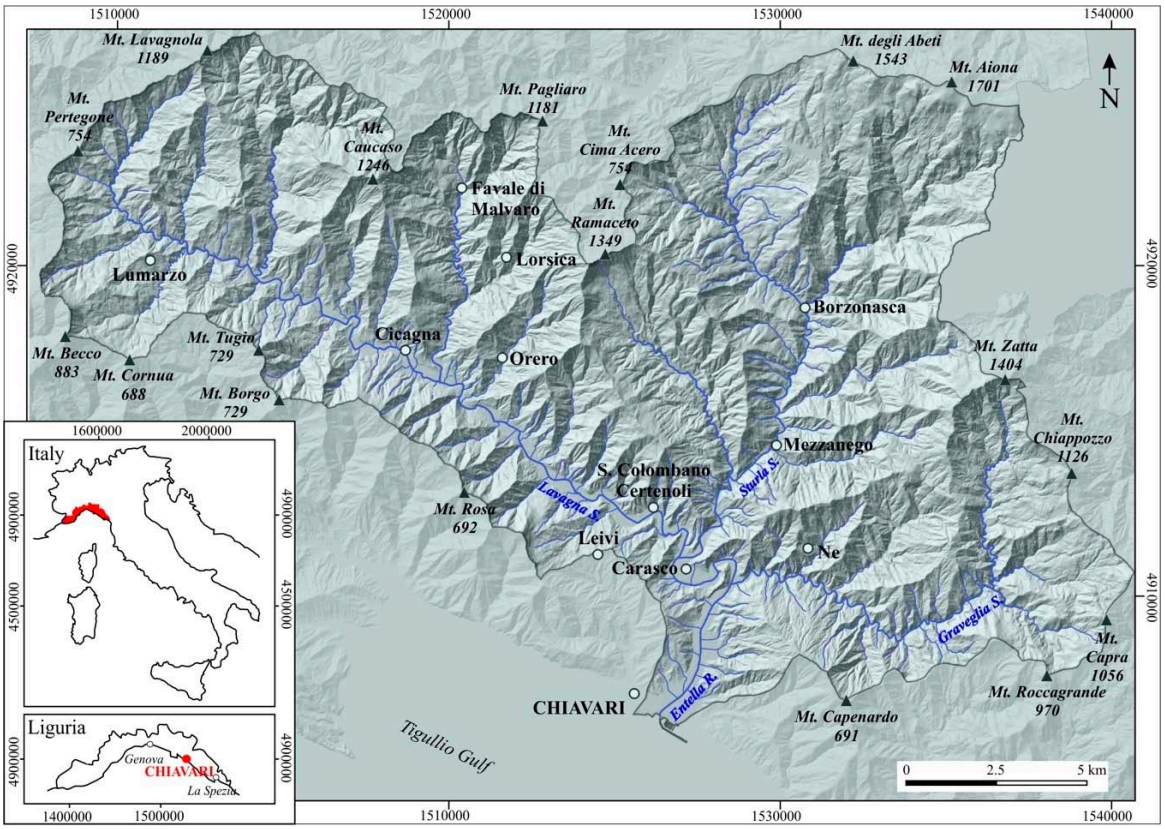

Figure 1. Geography of the Entella River basin.

In the catchment area, Jurassic to Paleocene rock types predominate; they are arranged in a complex geological setting (Figure 2), with multiple sets of tectonic discontinuities [68–71]. In detail, shale with sandstone and calcarenite layers (Scisti Zonati Fm.), shale and light grey limestone (Argille a Palombini Fm.), marl and silty-marl with shale or calcareous joints (Ardesie di Monte Verzi Fm.), and marly limestone and calcareous marl (Flysch di Monte Antola Fm.) crop out in the Lavagna and lower Sturla valleys, whereas thick sandstone layers (Arenarie del Gottero Fm.) form the Ramaceto and Zatta mounts. A typical ophiolite sequence encompassing serpentinite, gabbro, basalt, ophiolitic breccia, chert, grey limestone (Calcari a Calpionella Fm.) and shale (Argille a Palombini Fm.) crop out along the watershed between the Sturla and Graveglia valley and in the eastern sector of the basin.

Marly limestone, marl and clayey marl (Flysch di Ottone Fm.), heterogeneous and chaotic complexes, consisting of ophiolitic sandstone, polygenic breccia and olistoliths of basalt, serpentinite, gabbro, limestone and chert (Casanova Complex), crop out in the upper Sturla valley, along the Tyrrhenian-Po divide. The geological and structural settings strongly influence the morphology of the catchment characterized by high relief and sharp gradients. Hills and mountains have steep and very steep slopes, covered by deposits of variable thicknesses due to gravity and/or superficial waters; flat land occupies less than 5% of the territory and comprises recent and terraced alluvial deposits, both in valley floors and in the coastal floodplains. Lower steep slopes host large and deep-seated landslides, where small settlements are often located.

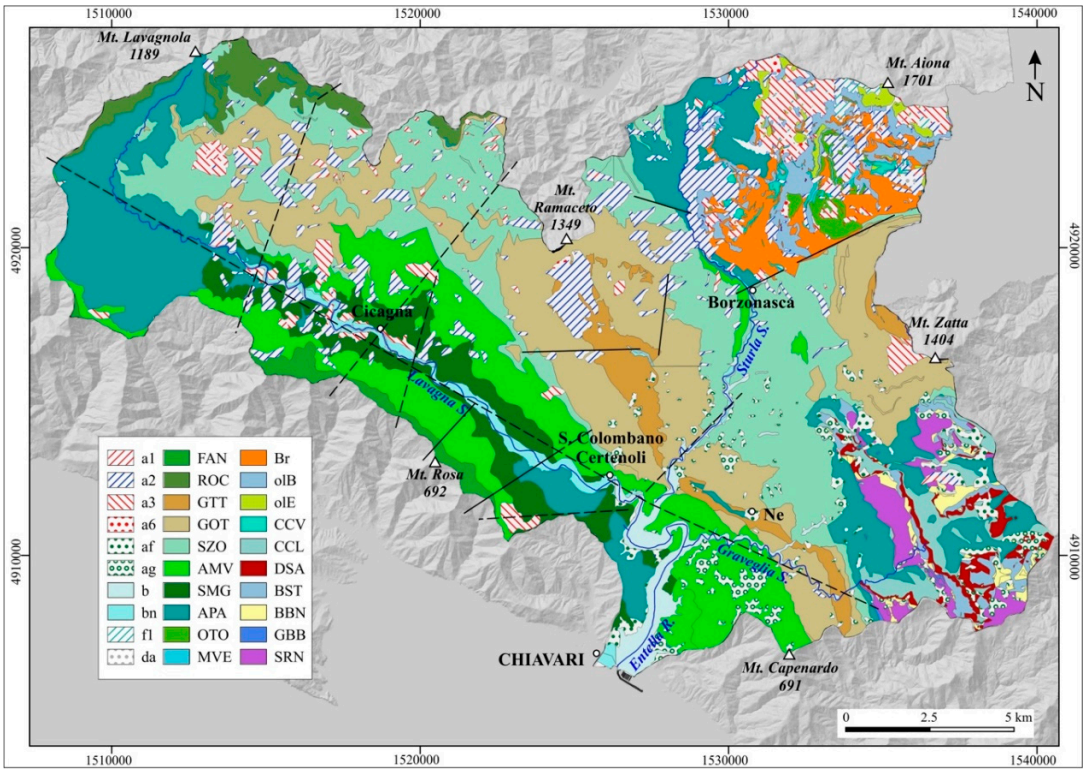

Figure 2. Geological sketch of the Entella River basin. Geological formations: a1, active landslides; a2, inactive landslides; a3, slope deposits; a6, rock debris; af, fine slope deposits; ag, granular slope deposits; b, recent alluvial deposits; bn, terraced alluvial deposits; f1, swamp deposits; da, anthropic deposits; FAN, Flysch di Monte Antola Fm.; ROC, Ronco Fm.; GTT, Argilliti di Giaiette Fm.; GOT, Arenarie del Gottero Fm.; SZO, Scisti Zonati Fm.; AMV, Ardesie di Monte Verzi Fm.; SMG, Scisti Manganesiferi Fm.; APA, Argille a Palombini Fm.; OTO, Flysch di Ottone Fm.; MVE, Complesso di Monte Veri Fm.; Br, Polygenic breccias; olB, Basalt Olistolites; olE, Ultrabasic Olistolites; CCV, Complesso di Casanova Fm.; CCL, Calcari a Calpionella Fm.; DSA, Diaspri d Monte Alpe Fm; BST, Basalts Fm.; BBN, Brecce; GBB, Gabbros Fm.; SRN, Serpentinites Fm. Black lines represent tectonic discontinuities.

Vegetated areas, natural or cultivated, largely cover the catchment area, with forests, pastures and small agricultural areas, including olive groves, chestnut woods and fruit orchards on well-maintained or abandoned terraces on the slopes. Artificial surfaces represent a small portion of the basin; built-up areas principally occupy the main valley floors and the coastal floodplain, whereas small and remote villages stand on the slopes. Outcrops of rocks with shrubs and herbaceous associations are common at high elevations.

The local morphology influences the climate conditions. The presence of valleys parallel (Lavagna and lower Graveglia valleys) and orthogonal (Sturla and upper Graveglia valleys) to the coast strongly influences the draft flow. Air masses and meteorological disturbances are channeled and pushed landward by southern winds against the Apennine ridge, parallel to the coast and locally exceeding

1700 m in elevation, favoring the formation of cloudbursts and thunderstorms which are characterized by intense and very intense rainfalls. The climate is Mediterranean, with dry and hot summers and relatively mild winters in which rainfall is abundant (from October to November and in February) [72]. Mean annual precipitation (MAP) averages 1750 mm and ranges from 1160 mm in the coastal floodplain to more than 2200 mm along the Tyrrhenian-Po divide.

2.2. Methods

A multi-temporal inventory of the ground effects on the slopes and damages induced by rainfall events in the Entella River catchment over the period 2000–2017 was implemented. We gathered landslide and damage information from different sources, e.g., newspapers articles and chronicle notes from local and social media (newspapers, TV, radio, internet), interviews with local inhabitants, damage reports and catalogues compiled by regional and local authorities, archives of local municipalities and, secondarily, scientific papers, technical and event reports. In particular, most of the landslide was acquired from online networks using both manual searches [73–75] and automatic web feed news aggregators, e.g., Google News or Google Alert [67]. Our search was performed by combining specific keywords, such as "landslide", "shallow landslide" related to other specific arguments, such as "rainfall" or "damage", and their Italian synonyms and words in both singular and plural forms. Each news item was checked for accuracy because the term "frana" (Italian word for 'landslide') can be used with different meanings. Furthermore, we excluded news relating to events which occurred outside of the considered temporal range (2000–2017), as some news was focused on mitigation actions related to older landslides. For each slope, the catalogue included: (i) the location of the landslide event, (ii) the administrative and geographical details, (iii) a short description of the ground effects observed on the slope, (iv) a brief report of the damage caused to assets, structures or people, and (v) information on the rainfall event that triggered the instability processes. Using different sources of information by terminology, accuracy and consistency standards, the data included in the catalogue are heterogeneous, and some therefore, causes of uncertainty are introduced. More commonly, a qualitative description of the instability phenomena was given, without objective evidence about the type, size or rate of the processes. Newspaper articles and chronicle notes report typically do not distinguish between shallow landslides, earth or debris flows, soil slips or rock falls, referring to them all as "landslides"; furthermore, unscientific expressions such as "massive landslide", "huge landslide" or, in case of rock falls, "enormous boulders" are commonly used to describe the size of the event. When the instability involves man-made structures (e.g., the subsidence or collapse of a road surface or retained wall), ground effects are often mistaken with the damage induced by the rainfall event. A further source of uncertainty is the accurate location of the landslides, particularly when cartographical documentation, with coordinates and altitude data, or detailed toponyms at least, are not available. One particular annotation concerns the damage catalogues and technical reports compiled by local authorities: in many cases, we observed that they include qualitative landslide information and approximate locations, according to different purposes, i.e., the assessment of damage and the associated emergency measures which were carried out.

The first step of the GIS-based approach we adopted was the integration of slope instability events in QGIS (QuantumGIS); since we have no areal information about landslide sizes, we adopted punctual features. When accurate information about location was available, we used latitude and longitude values quoted in technical reports to georeference slope failures; otherwise, when toponyms or road marks were included in newspaper articles or damage reports, we identified and manually georeferenced the approximate locations of the instability processes using either the regional technical maps listed in Table 1 or modern cartographical platforms (e.g., Google Earth, Google Maps and Google Street View). Geolocalizing based on information found in online networks using local place names, physiographic elements or sub-municipality localities result in a poor localization accuracy, and a source of uncertainty can be introduced.

Table 1. Overview of the regional maps used for the Entella basin's analysis.

Map	Scale	Year
Regional geological map, Table 232.3 Sestri Levante and 232.4 Lavagna	1:25,000	2004
Regional geological map, Table 231.1, 231.4 Chiavari-Recco	1:25,000	2005
Regional geological map, Table 215.3 Borzonasca	1:25,000	2006
Regional thematic map, slope aspect	1:5000 1:10,000	2007
Regional thematic map, slope steepness	1:10,000	2007
Regional thematic map, land-use	1:10,000	2015
Regional thematic map, landslides susceptibility	1:10,000	2017
Catalogue of landslides, IFFI (Inventario Fenomeni Franosi in Italia) Project	1:10,000	2014
Regional technical map, 3D topographical database	1:5000	2007

We stress the fact that the landslide dataset is not a thorough inventory map of landslide events, but rather, a set of georeferenced features that represent the distribution of instability processes induced by rainfalls observed on the slopes and their interference with human settlements or structures, gathered from heterogeneous and mainly qualitative information sources.

An analysis of the spatial relationships among rainfall-induced landslides and predisposing factors was carried out to evaluate the likelihood of a slope failure to occur. Using the set of regional technical and thematic maps listed in Table 1, a series of spatial analyses was performed to compare each slope instability phenomenon with the geological, geomorphological and land-use settings of the Entella River catchment. We selected the following geological, morphological, environmental and anthropogenic factors which influence the stability of the slopes and the occurrence of landslides, and we evaluated the incidence of slope movements according to these categories: lithology, slope aspect and steepness [39,73], drainage and land-use [39,76–78], man-made structure, e.g., distance from roads and buildings [39,76,77,79], and existing gravitational processes. At this stage, a new source of uncertainty has been introduced due to the modelling of the predisposing parameters used in the thematic maps that we acquired from the regional cartographical archives.

The different and heterogeneous lithological units in the regional geological maps at 1:25,000 scale (Table 1) were grouped and rearranged into 13 categories based on the litho-technical features of the bedrock (Figure 3). The dominant lithology included clayey flysch (40%), sandstone (18%), incoherent soils (15%) and slate (11%).

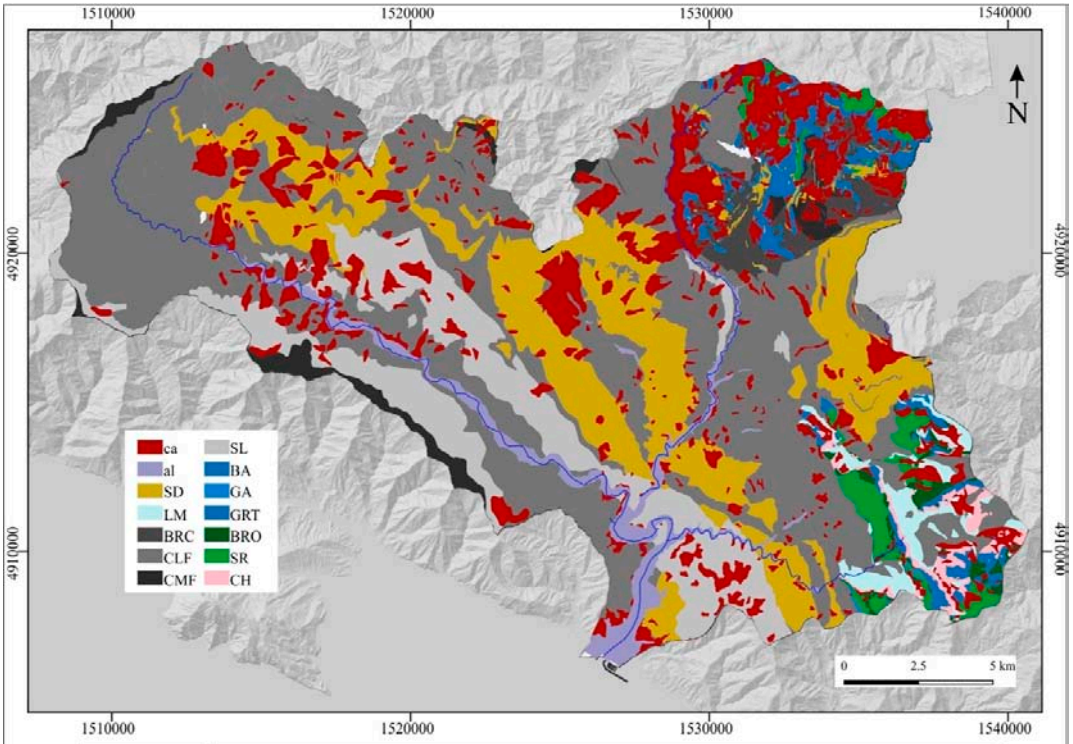

Class	Description
ca	Incoherent soils, including silt and clay with granular fraction and coarse soil mixed up with heterogeneous materials
al	Heterogeneous clayey and sandy deposits
SD	Sandstones
LM	Limestones
BRC	Clayey-pelitic breccias and olistolithes
CLF	Clayey flysch
CMF	Calcareous-marly flysch
SL	Slates
BA	Basalts
GA	Gabbros
GRT	Granites and granitoides
BRO	Heterogeneous breccias
SR	Serpentinites
CH	Cherts

Figure 3. Litho-technical map of the Entella River basin.

Slope aspect and steepness were derived from regional thematic maps at 1:10,000 scale (Table 1), where topographical parameters are given in numerical ranges: the slope aspect has been classified into 8 categories (in degrees), coinciding with geographic directions (Figure 4A), whereas the slope steepness was classified into 6 categories (in percentage), from "very low" (0–10%) to "very high (>75%) (Figure 4B). Most of the slopes in the catchment area are south oriented, (south-west, 15%; south. 13%; south-east, 12%), with high steepness (39%) ranging from 51% to 75%, and medium high steepness (23%).

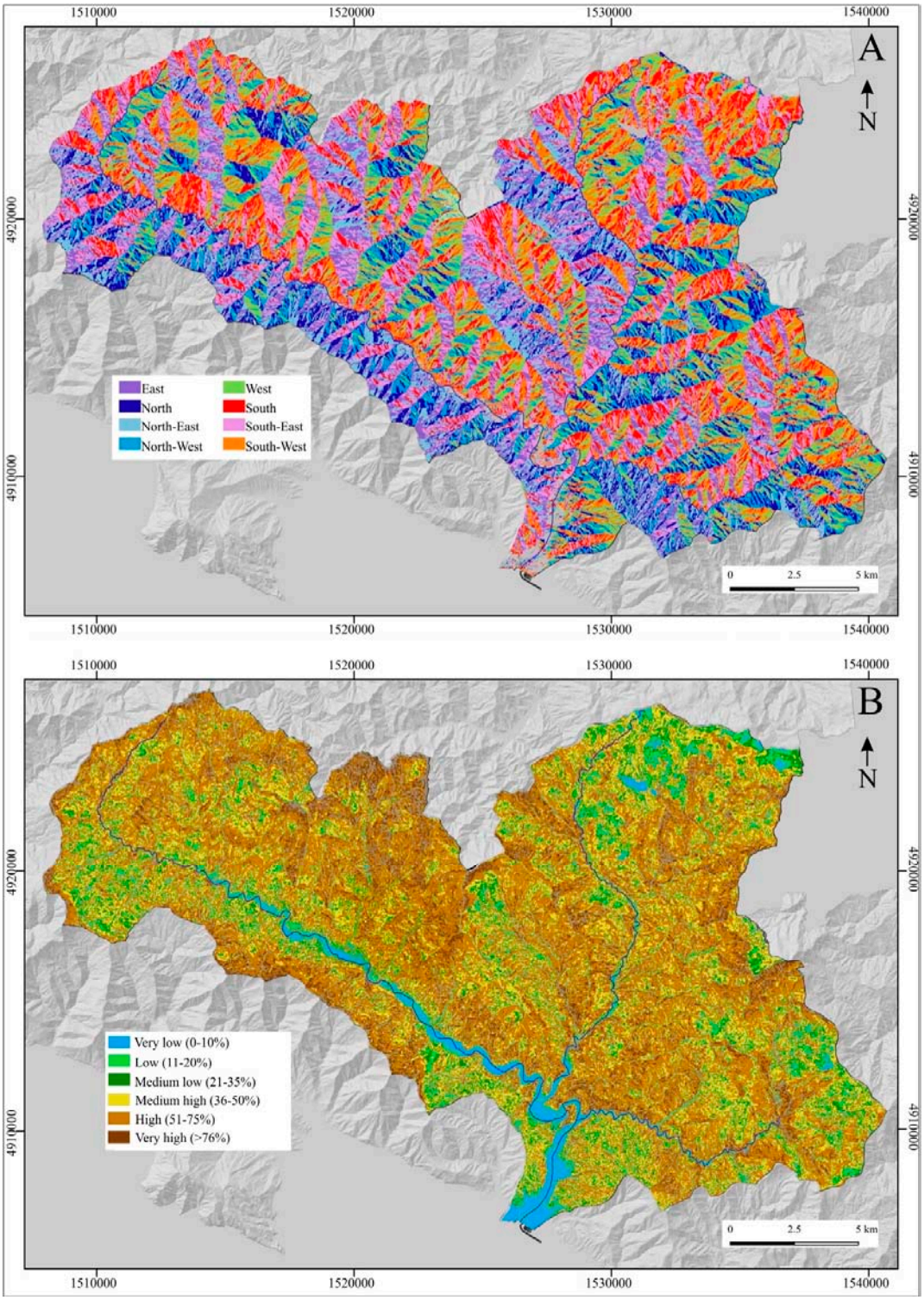

Figure 4. Thematic maps representative of the morphometric landslide predisposing factors: (**A**) slope aspect; (**B**) slope steepness.

Land-use information has been extracted from a regional thematic map at 1:10,000 scale (Table 1), which was properly rearranged and simplified with respect to the geo-hydrological risk responses and the local conditions of the Entella River catchment (Figure 5). The regional land-use map is composed by 45 categories according to the CO.RI.NE. (Coordination of Information on the Environment) land-use classification [80]. In order to reduce data redundancy, we grouped the units belonging to

the same land-use category, thereby obtaining 28 classes, while providing the relevant information in the database. The catchment area is occupied largely by forest (69%) and secondarily by natural vegetated spaces, including grassland, moors and shrubs (16%), various agricultural land (11%) and urban areas (4%).

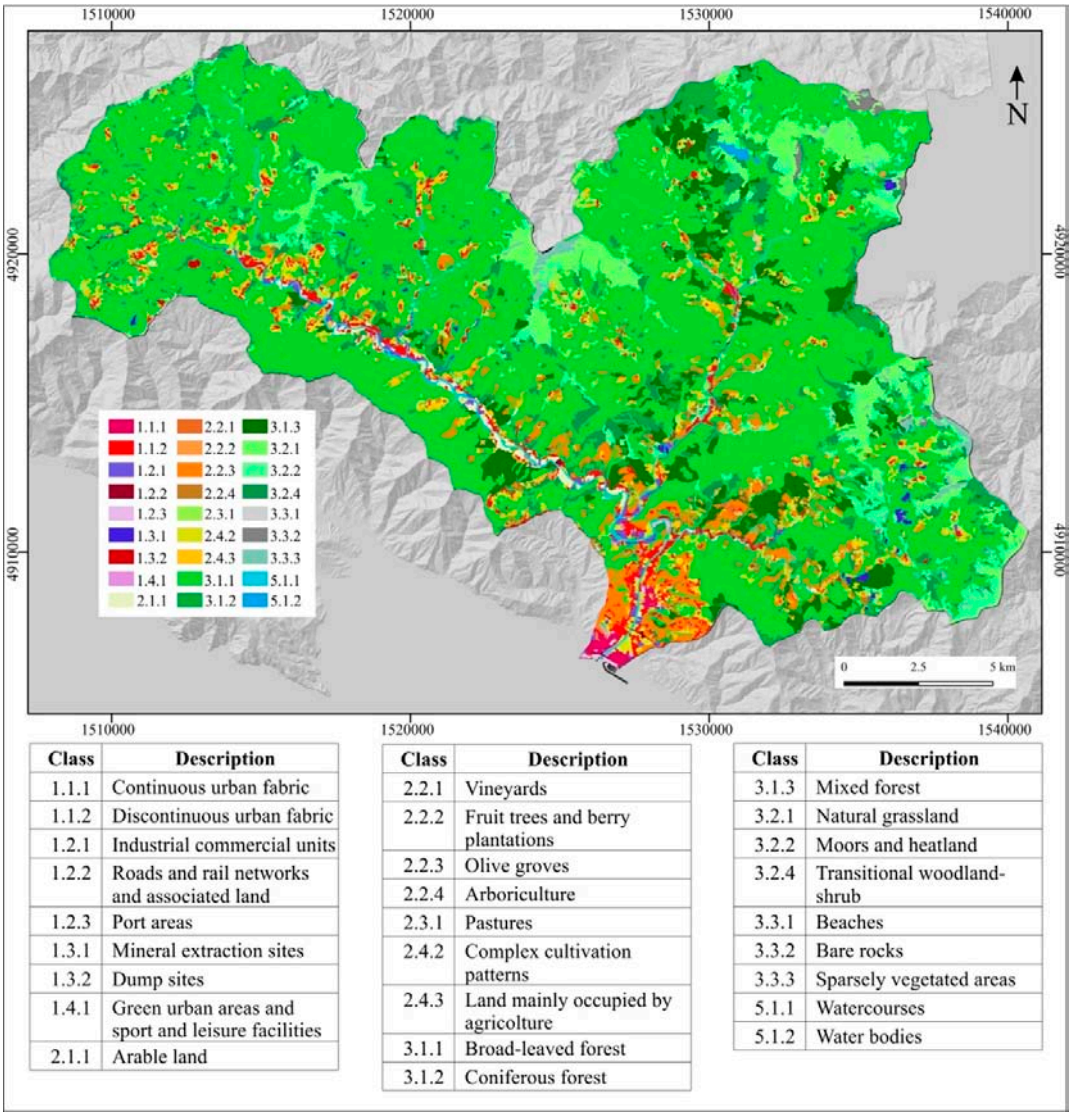

Class	Description
1.1.1	Continuous urban fabric
1.1.2	Discontinuous urban fabric
1.2.1	Industrial commercial units
1.2.2	Roads and rail networks and associated land
1.2.3	Port areas
1.3.1	Mineral extraction sites
1.3.2	Dump sites
1.4.1	Green urban areas and sport and leisure facilities
2.1.1	Arable land

Class	Description
2.2.1	Vineyards
2.2.2	Fruit trees and berry plantations
2.2.3	Olive groves
2.2.4	Arboriculture
2.3.1	Pastures
2.4.2	Complex cultivation patterns
2.4.3	Land mainly occupied by agricolture
3.1.1	Broad-leaved forest
3.1.2	Coniferous forest

Class	Description
3.1.3	Mixed forest
3.2.1	Natural grassland
3.2.2	Moors and heatland
3.2.4	Transitional woodland-shrub
3.3.1	Beaches
3.3.2	Bare rocks
3.3.3	Sparsely vegetated areas
5.1.1	Watercourses
5.1.2	Water bodies

Figure 5. Land-use map of the Entella River basin.

Map of drainage networks (Figure 6A) and anthropogenic elements, i.e., buildings, road networks and man-made structures (Figure 6B) have been extracted from the regional topographical database at a 1:5,000 scale (Table 1). We analyzed the influence of drainage networks on slope stability, taking into account the distance from roads, buildings and other man-made structures, e.g., retaining walls, artificial scarps or farming terraces with dry-stone walls, using surrounding buffers ranging from 1 to 500 m. To measure the distance from point and linear elements, such as springs, buildings, watercourses and roads, we used the minimum distance technique. Regarding polygonal elements, we considered the distance from their barycenter.

Existing landslides and gravitational processes were derived from the regional catalogue of landslides at 1:10,000 scale, in which landslides are mapped and classified on the basis of their state of activity (active/re-activated/suspended, dormant, stabilized) and type of movement (slow flow, rapid flow, complex, fall/topple, roto-translational slide, areas potentially affected by fall/toppling or

shallow landslides, deep-seated gravitational slope deformation). We stress the difference between this regional landslide inventory map, which includes detailed data derived from field surveys and technical reports, but which is not necessarily updated after each geo-hydrological event, and the landslides dataset used in this paper, which does not include quantitative data and mapping of the landslide areas because of the heterogeneous nature of the information sources with which it was constructed.

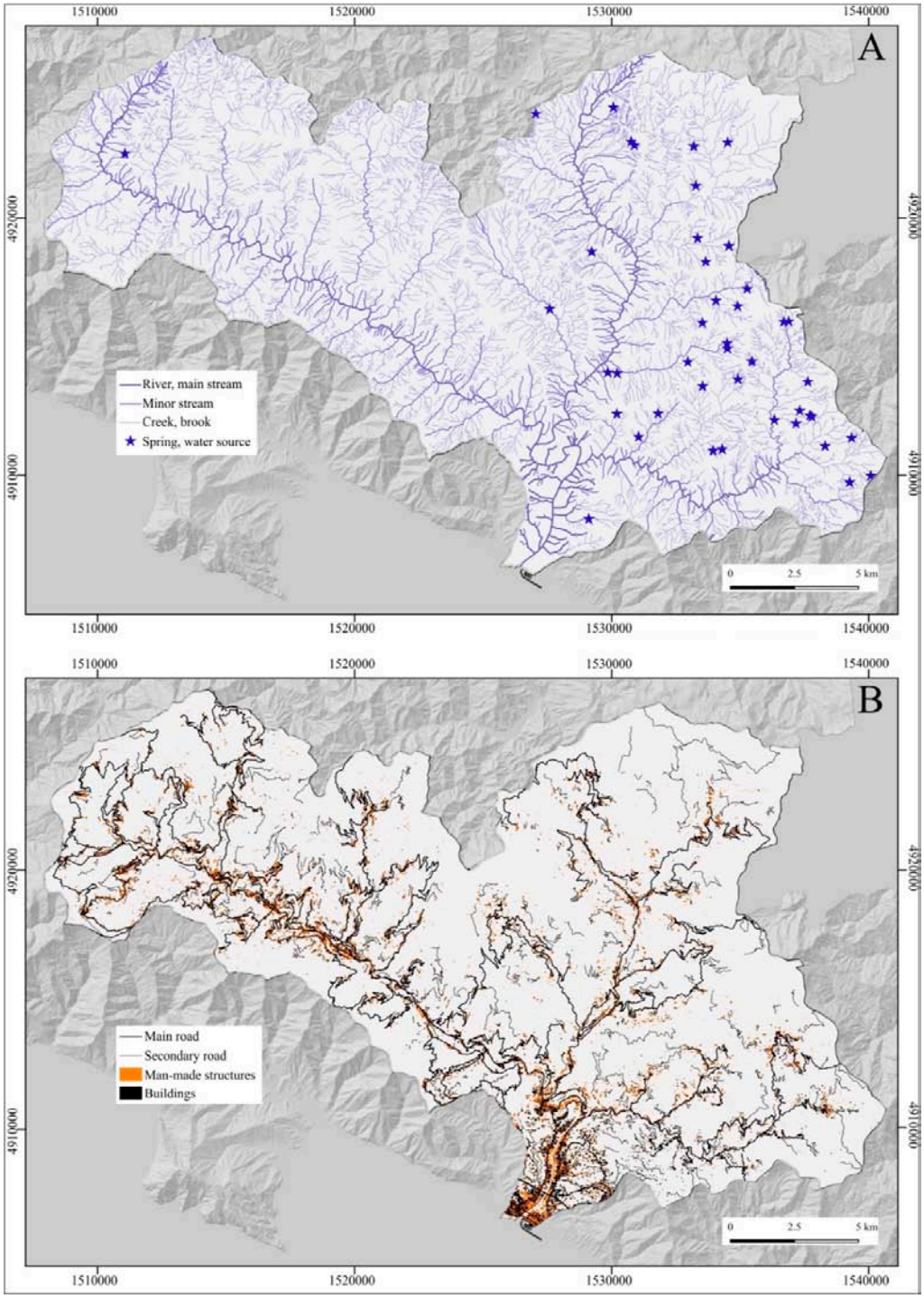

Figure 6. Thematic maps representative of the landslide predisposing factors: (**A**) drainage pattern; (**B**) anthropic elements (roads, buildings, retaining walls, artificial scarps, terraces and other man-made structures, etc.).

Next, we reclassified predisposing geological, morphological and environmental factors into four relevant classes, from low to very high, based on the statistical spatial distribution of instability processes in each category of the thematic layer. Then, we assigned a weighted value to each class which was proportionate to the spatial incidence of landslides in each category, ranging from 1 to 4 [75]. Using the same criteria, we associated a weight, ranging from 1 to 2, to the distance from drainage patterns, springs, roads, buildings, walls and man-made structures, based on the frequency of slope failures in different distance breaks. Regarding existing landslides mapped in the regional inventory, we added a further score, ranging from 1 to 4 for areas with no landslides, stable landslides, dormant landslides and active landslide respectively. Adopting a grid with a 25 × 25 m cell size, we overlaid the different layers associated with the predisposing factors, both natural and anthropic, and combined them in order to determine a rating in terms of slope instability proneness, calculated as the sum total of weights in each cell-grid. In addition to the accuracy of the punctual landslide input data and the predisposing parameters, further uncertainties were associated with (i) the resolution of the grid adopted in the spatial analysis, related to the extent of the catchment area, (ii) data combination and the extrapolation of the resulting value from the punctual landslide features to the corresponding cell-grid, and (iii) assessments of criteria weights which were subjectively defined on the basis of the statistical distribution of landslide features in each class.

Finally, we used total scores to propose a map of landslide-prone areas for the Entella catchment, with 5 tendency classes, i.e., from null to very high, which would take into account the influence of different predisposing factors vis-à-vis the occurrence of slope movements, including land-use and man-made disturbance.

In an attempt to assess the accuracy of the method and to perform a validation of the results, a test dataset was prepared using samples of rainfall-induced landslides which occurred over the period from 30 December 2017–5 February 2019. Landslide data were provided exclusively from online networks, including newspapers and local media, using both manual searches and web feed readers based on a combination of the aforementioned specific keywords and arguments.

3. Results

In the 2000–2017 period, we identified 45 rainfall events that caused large and widespread ground effects on the slopes in the Entella River catchment (Table 2). Using landslide information and damage notifications, we recognized 664 natural instability processes distributed among all the Municipalities inside the catchment area. Approximately 10% of the collected data were provided from newspaper and other online networks, 35% from technical reports and 55% from unpublished catalogues and reports compiled by local municipalities. The percentage of landslide news coming from the internet could easily have been greater than 30%, but most of the information matched georeferenced and more accurate notifications from local authorities; In this study, we opted for the latter where possible, at the expense of online sources. As illustrated in Figure 7, rainfall events mainly affected low-medium elevations and the central sector of the basin, including the lower Lavagna and Graveglia valleys and the middle-lower Sturla valley. The municipal district of Mezzanego (151) and Borzonasca (129) in the Sturla valley, San Colombano Certenoli (176) in the Lavagna valley, and Ne (93) in the Graveglia valley experienced the greatest number of criticalities and damage notifications (Table 3).

Table 2. Rainfall events that have caused shallow landslides and instability phenomena on the slopes in the Entella River basin in the 17-year period covering 2000–2017. Sites: BR, Borzonasca; CG, Cicagna; CR, Carasco; CV, Chiavari; CN, Cogorno; CL, Coreglia Ligure; FM, Favale di Malvaro; LM, Lumarzo; LR, Lorsica; LV, Leivi; MG, Mezzanego; MC, Moconesi; NE, Ne; NR, Neirone; OR, Orero; SC, San Colombano Certenoli; TR, Tribogna. See Figure 1 for location of the sites. Damaged element: B, building; I, infrastructure; R, road; S, structure; C, casualty.

#	Date	Site	Damage
1	6 November 2000	NE	R
2	24–26 November 2002	CR, LV, MG, NE, SC	C, S, I
3	31 October–1 November 2003	BR, NE	R, S, I
4	19–20 February 2006	BR	S, I
5	8 December 2006	BR	R
6	26 September 2007	NE	R
7	21–23 November 2007	CR, MG	R
8	19 April 2008	SC	R
9	11–12 November 2008	CR, NE	R, I
10	1–2 December 2008	CR, NE	R, S, I
11	20–22 January 2009	BR, CG, MG, NE	R, S, I
12	2 April 2009	BR	R
13	8 December 2009	CR	R, I
14	22–26 December 2009	BR, CR, MG, NE, OR	R, S, I
15	7 May 2010	NE, FM	R, I
16	1–3 November 2010	BR, MG, NE	R, S, I
17	22–24 December 2010	BR, MG	R, S, I
18	10 January 2011	BR	R
19	7–8 June 2011	NE	R
20	4–5 September 2011	NE	R, I
21	25 October 2011	NE	R
22	4–6 November 2011	NE	R
23	17–18 March 2013	MG	R, S, I
24	29 March 2013	CR	R
25	27 April 2013	TR	R
26	27 June 2013	NE	R
27	21–22 October 2013	BR, CR, LV, MG, NE, SC	C, R, S, I
28	30 October 2013	CG, CL, FM, MC, OR	R, S, I
29	3 November 2013	MG	R
30	25–26 December 2013	BR, CR, CG, LV, LM, MG, MC, NE, NR, TR	R, S, I
31	4–5 January 2014	BR, CR, MG, NE, TR	R, S, I
32	16–20 January 2014	BR, CR, LM, MG, MC, NE, SC, TR	R, S, I
33	9–11 February 2014	BR, MG, NE, SC	R, S
34	1–3 March 2014	BR, CR, LV, SC	R, I
35	10–11 October 2014	BR, CR, CG, CL, LR, LM, MG, MC, NE, NR, TR	R, S, I
36	3–6 November 2014	NE	R
37	10–11 November 2014	BR, CR, CV, CG, CN, FM, LV, MG, NE, SC	C, R, S, I
38	17 November 2014	FM, CG	R
39	22 January 2015	LR	R
40	14 September 2015	BR, CR, CG, FM, LR, SC	R, S, I
41	9 February 2016	LR	R
42	12 February 2016	LR, SC	R, S
43	23 February 2016	NE	R
44	12 December 2017	BR	R, I
45	26–28 December 2017	LM	R

Table 3. Distribution of geo-hydrological criticalities and damage notifications in the Municipalities inside the Entella River basin over the 17-year period from 2000–2017. See Figure 1 for the location of the listed sites.

Municipality	Basin	#
Borzonasca	Sturla	129
Carasco	Sturla	38
Chiavari	Entella	1
Cicagna	Lavagna	15
Cogorno	Entella	1
Coreglia Ligure	Lavagna	2
Favale di Malvaro	Lavagna	14
Leivi	Lavagna	13
Lorsica	Lavagna	5
Lumarzo	Lavagna	10
Mezzanego	Sturla	151
Moconesi	Lavagna	10
Ne	Graveglia	93
Neirone	Lavagna	6
Orero	Lavagna	4
San Colombano Certenoli	Lavagna	176
Tribogna	Lavagna	8

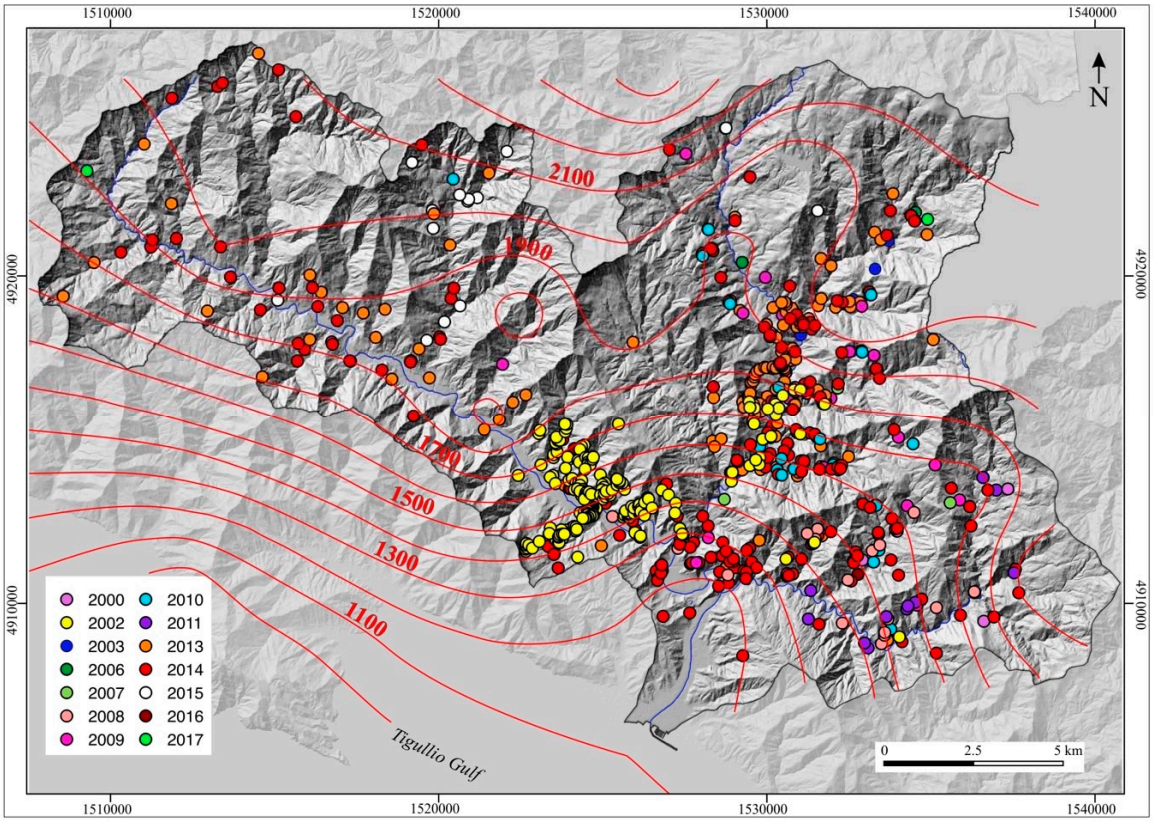

Figure 7. Spatial distribution of rainfall-induced shallow landslides which occurred in the Entella River basin over the period from 2000–2017. Red curves show the distribution of the mean annual precipitation in the catchment area.

Ground effects induced by heavy rainfalls included widespread shallow landslides, primarily soil slips [81], slow-moving earth flows and rapid to extremely rapid mud flows [16,17], and rock-falls (Figure 8). Slope failures chiefly involved colluvial deposits and reworked debris covers of variable thicknesses, and the superficial portions of weathered and fractured bedrock. Large volumes of

water mixed with mud, debris and vegetation, including materials resulting from the destruction of agricultural terraces, were mobilized along the slopes and thalwegs; blocks collapsed from vertical or sub-vertical rock walls upstream of road corridors and buildings. In many cases, processes have not been classified due to the lack of accurate information and technical details.

Types of common damage ranged from soil disruption to debris or mud deposition along streams and roads, subsidence and removal of sections of roads or pedestrian paths, collapse of retaining walls and artificial scarps, causing the interruption of services and/or the demolition of structures and infrastructure, and at some locations, the destruction of buildings and warehouses (Figure 8).

Figure 8. Examples of the different types of shallow landslides induced by rainfalls and the resulting damage: (**A**), roto-translational slide; (**B**), rotational slide downhill road cuttings, resulting in the partial collapse of the roadway; (**C**), shallow landslides on terraced slopes, with the collapse of the retaining walls; (**D**), complex movement uphill road cuttings, resulting in the roadway obstruction due to debris, blocks and vegetation; (**E**), rockfall; (**F**,**H**), soil slips and slow-moving earth flows, resulting in significant damage to buildings and man-made structures due to mud and debris; (**G**), rapid earth flow.

An analysis of the spatial distribution of these sets of landslides in different litho-technical classes shows that slope failures occurred mainly in clayey flysch, CLF (61%), and slates, SL (23%), whereas incoherent soils and debris covers, sandstone, heterogeneous and ophiolitic bedrocks, were affected by instability phenomena to a lesser extent (Figure 9A).

By evaluating the statistical distribution of landslides with respect to the two morphometric parameters considered (i.e., slope aspect and steepness), slopes of south-east (18%) direction are largely affected by gravitational processes induced by rainfall events; south (17%), south-west (16%) and west (15%) are also relevant slope directions, whereas slopes of north-east (9%) and north (7%) directions are

rarely involved in instability phenomena (Figure 9B). Failures affected mainly slopes with high (42%) and to a lesser extent, with medium-high (28%), steepness values (Figure 9C). Most of the unstable areas have slope steepnesses ranging from 36% to 75%.

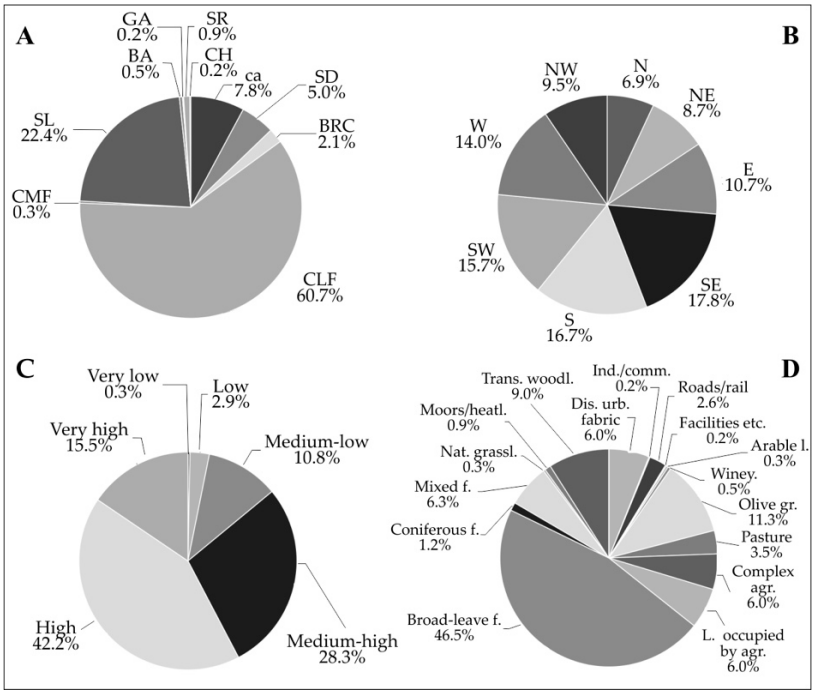

Figure 9. Statistical distribution of predisposing factors in areas affected by landslides in the Entella River basin: (**A**), lithology; (**B**), slope aspect; (**C**), slope steepness; (**D**), land-use.

Most of the gravitational processes (91%) occurred on uninhabited and/or, at first glance, natural slopes, covered by forests (53%) and, secondarily, on agricultural (26%) and natural vegetation (10%); in 9% of cases, instability events involved urban areas. In particular, landslides developed mainly within broad-leaved forests (46%), followed by olive groves (11%) and transitional woodland/shrub (9%) (Figure 9D). A significant percentage of landslides (10%) were observed on terraced slopes, made of dry-stone walls terraces or grassy embankments which were mainly cultivated with olive groves and vineyards, including both well-maintained (89%) and abandoned or untended (11%) lands. Regarding artificial surfaces, slope instability occurred within discontinuous urban fabric (6%) and along road networks (3%).

The observed instability processes and existing landslides, mapped and classified in regional master plans, match in 19% of cases (Figure 10A). Instability occurred on slopes affected by active landslides (53%), with complex (43%) and roto-translational slides (35%) movement; rapid flows accounted for 13%. Furthermore, the percentage of instability phenomena corresponding to existing gravitational processes increased to 41%, if we consider a buffer around the landslide features, setting a distance of 50 m.

The results of a spatial analysis between rainfall-induced landslides and drainage patterns are shown in Figure 10B. We found that 16% of landslides occurred within 10 m from watercourses, and only in a few cases (2%) along drainage patterns. Similarly, instability processes were detected along main and secondary road networks in 4% and 2% of cases, respectively (Figure 10C). More than 40% of landslides were observed at a distance greater than 100 m from road infrastructure, although this does not exclude a possible interaction with the road network and the damaging effects on it (Figure 8).

Despite the fact that most of the slope movements occurred on uninhabited and/or, at first glance, natural slopes, anthropic elements, such as rural buildings, huts, artificial scarps or retaining walls, etc., they also occurred on mainly vegetated slopes, with a possible interactions between landslides

and man-made structures. Considering a buffer of 50 m around the landslide features, in most cases, failures occurred at a distance greater than 50 m from buildings (65%), including sheds, churches, rural or general buildings (Figure 10E), and from other man-made structures (66%) including huts, ruins, cisterns, shelters, burial grounds, monuments or pools (Figure 10F). In contrast, 76% of the gravitational processes were observed within 50 m of retaining fences and structures, included retaining walls, artificial scarps and dry-wall farming terraces (Figure 10D).

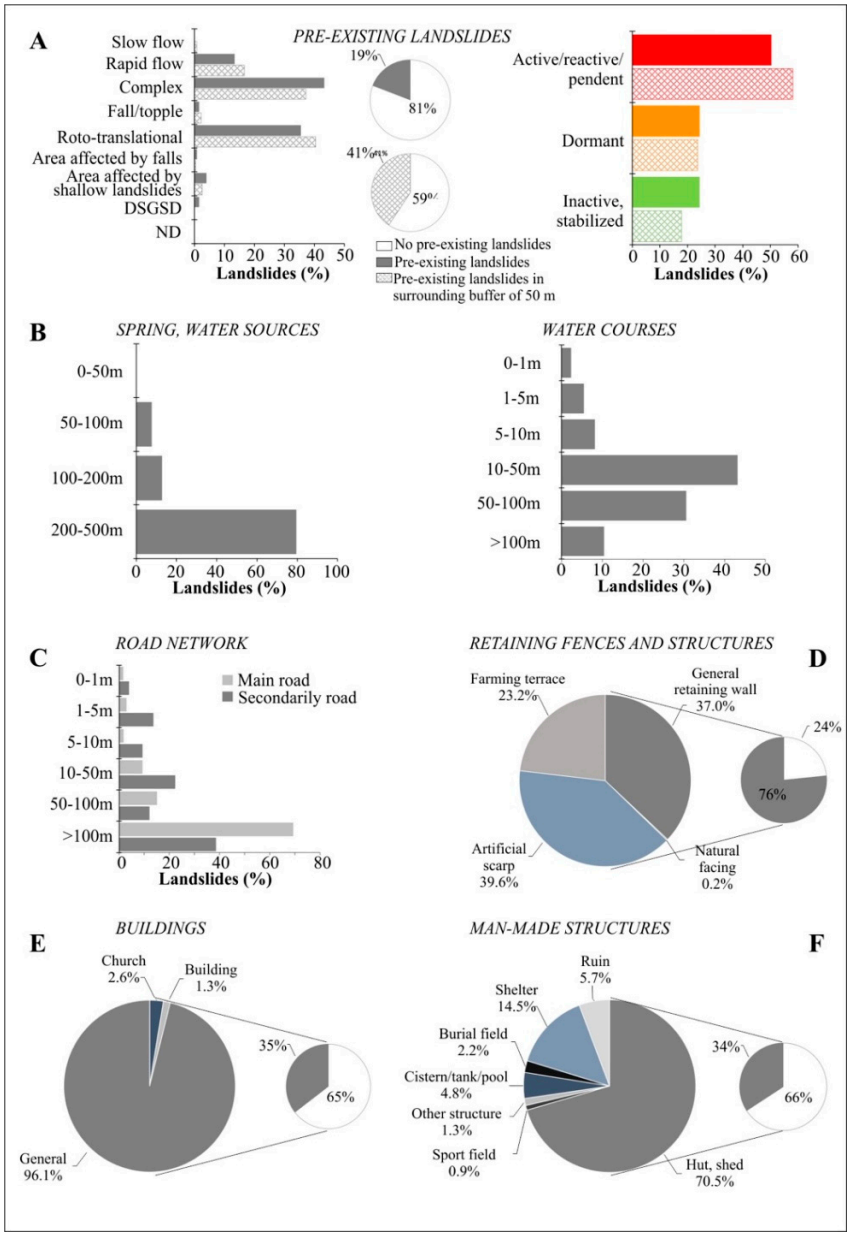

Figure 10. Statistical distribution of landslides regards to the geomorphological, hydrological and anthropic settings of the Entella catchment area: (**A**), pre-existing landslides; (**B**), drainage patterns, including springs and watercourses; (**C**), road network; (**D**), retaining fences and structures; (**E**), buildings and (**F**) other man-made structures.

Relating to the regional landslide susceptibility maps at 1:10,000 scale (Table 1) which are currently used by local authorities and decision makers for land-planning and risk management, most of the observed instability phenomena (50%) lies in the "high susceptibility, S3b" class (including dormant

or inactive/stabilized landslides), followed by "medium category, S1" (26%), whereas in 9% of cases, failures involved slopes classified as "very high susceptibility, S4" (including active landslides).

By evaluating the spatial distribution of the selected landslides in the different categories of the thematic layers (Figure 9), we reclassified the lithological, morphometric and environmental parameters using different classes, from "low" to "very high" (Tables 4–6).

Table 4. Reclassification of the lithological categories based on the statistical distribution of landslides (%) (see also Figure 9) related to the litho-technical features of different materials and their extent in the catchment area.

Spatial Distribution of Landslides (%)	Lithological Category	Litho-Technical Category	Class
<1	Alluvial deposits (al)	Heterogeneous clayey and sandy deposits	Low
	Basalts (BA) Gabbros (GA) Polygenic sedimentary ophiolitic breccias (BRO) Serpentinites (SR)	Ophiolitic rocks	
	Cherts (CH)	Siliceous rocks	
	Granites and granitoids (GRT)	Intrusive and massive metamorphic rocks	
	Limestones (LM)	Mainly calcareous rocks	
	Calcareous-marly flysch (CMF)	Heterogeneous sequences and chaotic complex	
1–5	Sandstones (SD) Clayey-pelitic breccias and olistolithes (BRC)	Mainly ruditic and arenitic rocks Heterogeneous sequences and chaotic complex	Medium
5–10	Incoherent soils (ca)	Incoherent soils, included silt and clay with granular fraction and coarse soil mixed up with heterogeneous materials	High
>10	Clayey flysch (CLF) Slates (SL)	Heterogeneous sequences and chaotic complex	Very high

Table 5. Reclassification of the slope aspect and steepness values based on the spatial distribution of landslides in each category of slope steepness and aspect (%).

Spatial Distribution of Landslides (%)	Steepness	Class
<1	0–10%	Low
1–15	11–35%	Medium
15–25	>76%	High
>25	36–75%	Very high
Spatial Distribution of Landslides (%)	**Aspect**	**Class**
<10	N, NE, NW	Low
11–13	E	Medium
14–15	W	High
>16	S, SE, SW	Very high

Table 6. Reclassification of the land-use units based on the spatial distribution of landslides (%) in each category, ordered according to increasing values.

Spatial Distribution of Landslides (%)	Land-Use Category	Class
<5	Continuous urban fabric Port areas Mineral extraction and dump sites Fruit trees and plantations Arboriculture Beaches Bare rocks Industrial and commercial units Green areas and sport leisure facilities Arable lands Natural grassland Vineyards Moors and headland Coniferous forests Roads and rail networks and associated lands Pastures	Low
5–10	Complex agricultural pattern Discontinuous urban fabric Land mainly occupied by agriculture Mixed forests Transitional woodland-shrubs	Medium
10–40	Olive groves	High
>40%	Broad-leaved forests	Very high

Heuristically selected weights [75,81] were associated with each predisposing parameter, as shown in Table 7. Scores ranged from 1 to 4, according to the incidence of landslides (in percentage) in each category of the thematic layer. For lithology, the highest score (4) was assigned to heterogeneous sequences and chaotic complexes, including flysch and slates; high (3) and medium (2) scores were assigned to slope covers and sandstone and heterogeneous breccias respectively, whereas the lowest score (1) was assigned to the remaining lithological classes, including ophiolitic, siliceous, intrusive and calcareous rocks. Based on the frequency distribution of landslides, the highest score (4) for the two morphometric parameters was associated with slopes oriented to the south (from south-east to south-west) and with steepness values ranging from 35% to 75% respectively; the minimum score (1) was assigned to hillslopes facing north or with steepness values below 10%. Regarding land-use, the category with the highest incidence of landslides, and therefore, with the highest susceptibility to instability, was broad-leaved forest (highest score, 4) followed by olive groves (high score, 3).

Table 7. Weights associated with each unit in the thematic maps, based on the incidence of landslides in the different categories. For the lithology, slope aspect, steepness and land-use classes, scores ranged from 1 ("low" category in Tables 4–6) to 4 ("very high" category in Tables 4–6).

Unit	Category	Weight
Lithology	Alluvial deposits	1
	Basalts	1
	Calcareous-marly flysch	1
	Cherts	1
	Clayey flysch	4
	Clayey-pelitic breccias and olistolites	2
	Gabbros	1
	Granites and granitoids	1
	Incoherent soils	3
	Limestones	1
	Polygenic sedimentary ophiolitic breccias	1
	Sandstones	2
	Slates	4
	Serpentinites	1
Slope aspect	N	1
	NE	1
	E	2
	SE	4
	S	4
	SW	4
	W	3
	NW	1
Slope steepness	0–10%	1
	10–35%	2
	35–75%	4
	>75%	3
Land-use	Arable land	1
	Arboriculture	1
	Bare rocks	1
	Beaches	1
	Broad-leaved forest	4
	Complex agricultural pattern	2
	Coniferous forest	1
	Continuous urban fabric	1
	Discontinuous urban fabric	2
	Dumps sites	1
	Green urban areas, sport and leisure facilities	1
	Industrial and commercial units	1
	Land mainly occupied by agriculture	2
	Mineral extraction sites	1
	Mixed forest	2
	Moors and headland	1
	Natural grassland	1
	Olive grove	3
	Pasture	1
	Port areas	1
	Roads and railway network	1
	Transitional woodland/shrub	2
	Vineyard	1

Similarly, we assigned weights to the spatial relationships with watercourses, road networks, buildings, other man-made structures and walls: weight values ranged from 1 to 2 based on the

incidence of landslides in the different spatial breaks (Table 8). We overlaid a further score ranging from 1 for areas with no landslides, to 4 for existing active landslides mapped in the regional inventory.

Table 8. Weights associated with each unit in the thematic maps, based on the incidence of landslides in the different categories. For existing landslides, springs, watercourses and anthropic elements, scores ranged from 1 (low incidence of landslides) to 2 or 4 (high incidence of landslides), depending on the number of adopted classes.

	Classes	Weight
Existing landslides	Stable areas	1
	Existing inactive/stabilized landslides	2
	Existing dormant landslides	3
	Existing active/reactive/pendent landslides	4
Springs	Distance < 50 m	1
	Distance > 50 m	2
Watercourses	Distance < 10 m	1
	Distance > 10 m	2
Anthropic elements	Roads < 5 m	1
	Roads > 5 m	2
	Buildings < 50 m	1
	Buildings > 50 m	2
	Man-made structures < 50 m	1
	Man-made structures > 50 m	2
	Retaining fencings and structures < 50 m	2
	Retaining fencings and structures > 50 m	1

Using a 25 × 25 m grid, thematic maps and predisposing parameters were combined. Through the summation of the different weights included in each cell-grid, a score in terms of susceptibility to the occurrence of a landslide was obtained. We derived the raster map, with a spatial resolution of 25 m, illustrated in Figure 11; it shows the degree of susceptibility to instability processes in the Entella River basin, according to classification into 5 levels, from null to very high (Table 9). To divide areas into different classes, we adopted a criterion based on the score ranges which were most representative for the value obtained in each cell-grid, supported by morphological settings and classification of the predisposing parameters, for the classes null, low and very high; median values were divided into two equal-sized classes.

Table 9. Classes of landslide proneness and their spatial distribution in the Entella River catchment area.

#	Class	Score	Area (km^2)
1	Null	1–14	8.73
2	Low	14–18	44.15
3	Medium	18–21	126.44
4	High	21–24	153.99
5	Very high	24–29	37.33

Most of the catchment area is characterized by high (42%) and very high (10%) levels of susceptibility to landslides; less than 15% is included in the low and null classes. By overlaying thematic layers on the obtained map, we observed that the highest classes (from high to very high) include hillslopes with south, south-east and south-west directions and steepnesses of between 35–75%, covered by bread-leaved forest on a bedrock mainly characterized by slate and clayey flysch, with no existing landslides, and characterized by the presence of man-made elements, such as retaining walls, artificial scarps and farming terraces.

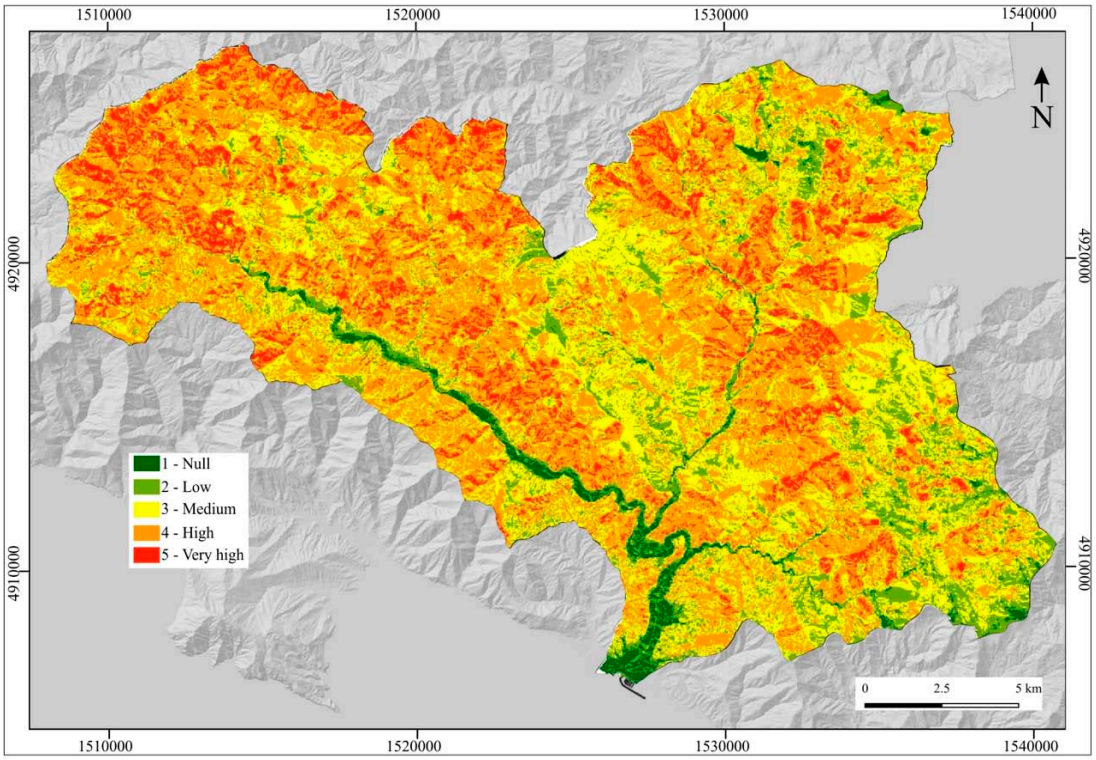

Figure 11. Map of the landslide prone areas of the Entella River catchment obtained using all the predisposing factors, including man-made elements and existing landslides.

As mentioned above, a susceptibility assessment was carried out using a test dataset which included new landslides observed in the catchment area. By comparing the landslide prone areas map and the distribution of the new samples, we detected new slope failures in areas of high (5 cases), medium (2 cases) and very high (1 case) risk of landsliding. In according with our findings, the new instability phenomena have been observed in slate (3 cases) and clayey-marl flysch (2 cases) and sandstone (3 cases), on slopes south-facing (SE and SW, 3 cases respectively; S, 1 case) with high steepness (35–75% in 7 cases) and in lands mainly occupied by broad-leave forests (5 cases). Most events occurred within 50 m from retaining walls or dry-wall terraces (8 cases), whereas roads, buildings and other man-made structures are at distances greater than 5 and 50 m respectively, but usually less than 100 m; water courses and springs are usually at distances greater than 50 m. We highlight that new slope failures involve slopes where existing landslides have not been mapped in the regional inventory and master plans (8 cases).

4. Discussion

The results obtained by the comparative analysis performed between the distribution of landslides and ground effects on slopes induced by rainfall events, and the geological, morphological, land-use and anthropic elements in the catchment area, allowed us to define the natural instability phenomena that affected the Entella River basin over the 2000–2017 period. Furthermore, the complex interplay among different predisposing factors for gravitational processes (i.e., lithology, slope steepness and orientation, land-use, drainage patterns and man-made disturbances) has been assessed. Widespread shallow landslides, soil slips, slow-moving earth flows, rapid to extremely rapid mud flows, and rock falls affected large portion of hillslopes, particularly in the central sector of the catchment in the lower Lavagna and Sturla valley, where the highest annual mean rainfall values are observed.

The geological and morphological settings of the catchment area represent the main predisposing factors for the triggering of rainfall-induced landslides: a significant relationship between lithology, slope aspect and steepness, and instability processes in the Entella River basin was observed, according

to other examples in literature [13,77,82]. Lithological heterogeneous sequences and chaotic complexes with a very high susceptibility to the development of landslides account for 80% of damaging events. Moreover, our findings highlight a link between landslide occurrence and anthropic structures, as reported by other authors [59,60,62,77,83]. More than 70% of the instability phenomena were observed within 50 m of retaining walls, including bench structures with dry-stone walls and edge-structures without stone walls and artificial scarps, and 50% within 50 m of buildings or other man-made structures. It is important to underline that in almost all cases, it was impossible to map where the movement started, due to the source of the landslide information. That means that landslides can be initiated close or very close to drainage networks, roads or other anthropic elements.

Failures generally affected natural or semi-natural slopes, which were either vegetated or inhabited. Nevertheless, anthropic elements, such as roads, buildings or other man-made structures, may frequently represent the sources of the failure. Slope failures occurred both upstream and downstream from roads scarps and/or the roadway surfaces, partially or totally interrupting and/or destroying infrastructure. The construction of these road networks is common in recent times, in order to connect isolated villages and to speed up connections with urban areas, motorways and the major road network that is located along the coastline. Starting from the 1960s and 70s, inland and rural regions were affected by an uncontrolled urban sprawl due to a population increase and the consequent demand for new areas to inhabit [63]. In many cases, this manifested in the enlargement of pre-existing paths or mule tracks, without particular attention to the regulation of run-off waters and slope re-profiling. Within this context, communication lines decrease slope stability and significantly increase the likelihood of occurrence of shallow landslides.

With regards to the relationship between land-use and instability processes, artificial surfaces correlate to an increase of landslides risk [59,81,84]; roads, buildings, structures, infrastructure and small villages cause a general reduction of soil permeability and induce negative effects on the natural drainage systems and on slope stability. In contrast, pasture and agricultural areas, including olive groves, vineyards, orchards, permanent crops and complex cultivation patterns, maintain the slope stability and contribute to the regulation of rainfall runoff. Cultivated and terraced agricultural areas with different degrees of maintenance play different roles on landslide susceptibility [60,61,85]. We observed that landslides affected both abandoned and cultivated terraced areas. According to the results obtained by other authors in different catchments characterized by agricultural practices [60,77], abandoned or poorly-maintained terraces are more frequently involved by instability phenomena. Negligible attention to the regulation of water runoff and inadequate preservation of man-made embankments and the dry-retaining walls that often collapse contribute to failures and increase the geo-hydrological risk. Natural vegetated areas, including forests and transitional woodland-scrub, represent potentially abandoned areas, where large shallow landslides initiate. Shrubs and herbaceous vegetation, and open spaces with little or no plants, favor erosional processes and an increase in sediment flow along minor watercourses. In a few cases, shallow landslides, mud flows and soil-slips have directly affected urban settlements or industrial sites, causing severe damage to structures and people, as was the case during the November 2014 rainfall event, when buildings, structures and facilities suffered extensive damage from numerous debris flows that affected the Leivi slopes, downstream from the confluence of the Lavagna and Sturla streams. At the toe of the slope, a long section of the municipal road was buried by debris and mud; a station for water supply was partially damaged, causing a prolonged interruption of water distribution; and a house was hit and entirely destroyed, causing two fatalities [66].

Most of the instability processes which occurred between 2000 and 2017 affected slopes that are stable or where no existing landslides had previously been detected or mapped. This is a significant result in terms of land-planning and risk management, because it points out that larger portions of territory and the population than expected are potentially at risk, with consequent extensive damage and high costs in economic, environmental and social terms. Regarding the comparison between the susceptibility map of the regional master plan and the map of the landslide-prone area obtained for

the Entella River catchment, we noticed that the small areas classified as showing very high levels of susceptibility overlay existing active/re-activated/suspended landslides. By evaluating all the predisposing factors, including human disturbance, we found that areas characterized by very high tendencies for landslides are more spatially distributed over the territory, and are made up of slopes where land-use and man-made structures, such as roads, terraces and buildings, may negatively influence slope stability. Similarly, areas with a high susceptibility to sliding include wide portions of hillslopes that have a higher predispositions to instability phenomena due to lithology, aspect, land-use or anthropic disturbance, in addition to existing dormant gravitational processes.

5. Conclusions

In recent decades, the Liguria region has been among the most affected Italian and Mediterranean hilly areas by rainfall-induced shallow landslides. In this paper, we present the case of the Entella River basin, a Tyrrhenian sector of the Ligurian Apennine: in the 2000–2017 period, a total of 45 rainfall events occurred, causing more than 664 damaging instability processes along the slopes. Starting from landslide information mainly from online networks and damage reports, an inventory of instability processes and ground effects induced by rainfall events in the study area was compiled and georeferenced. A series of comparative analyses was performed to define the role played by different predisposing factors, both natural and anthropic, and their influence on instability processes. The tendency for sliding was assessed by implementing a simplified-qualitative GIS-based approach based on ten predisposing factors, including anthropic elements (i.e., lithology, slope aspect, steepness, land-use, existing landslides, distance from watercourses and natural springs, buildings, road networks and retaining structures), weighted according to the spatial distribution of landslides in different classes. A map of landslide prone areas was produced. Although we adopted a semi-quantitative approach based on the combination of different predisposing parameters and unstructured data, we created a reliable assessment of the likelihood for landslides in the study area, as provided by the validation procedure using an independent set of new landslides observed in the period from 2018–2019.

The short duration, intense rainfall events that frequently affected the basin, together with the severe morphological conditions and human activity that has progressively and intensively modified the landscape in recent decades, resulted in higher incidence of landslides. Instability affected generally natural or semi-natural slopes, vegetated and, at first glance, inhabited; however, gravitational processes occurred frequently where anthropic elements exist. We identified a significant link between anthropic landforms and slope instability. The extensive and widespread damage framework shows good correlation with the road networks, buildings, terraces and other man-made structures, and can be correlated with the unplanned urbanization that took place over recent decades on slopes characterized by a basic high tendency for instability due to the morphological and geological features. The results of this study highlight the influence of human activity on landslide occurrence: re-profiling the slope and modification of the landscape increase the likelihood that a landslide will occur.

Although most of the observed processes are included in the high category in the regional susceptibility map, a considerable number of them affected slopes with a medium and low susceptibility level and numerous shallow landslides have been observed where no existing processes were mapped. Our findings highlight that the method generally adopted in land-planning for landslide susceptibility and risk assessment needs to be improved. Analysis of ground effects and the damage induced by instability processes, land-use changes and the influence of man-made elements on the slope stability and the occurrence of landslides have to be taken into account on regional-scale landslide risk assessment. Starting from landslide and damage information, which is easy to find and manage, a simplified-qualitative GIS-based approach for assessing and mapping susceptibility to instability was presented. It provides a useful tool for land planning to support local governments and all stakeholders in identifying areas characterized as being at high risk, and in recognizing the priorities for the plan of the most appropriate measures and urban resolutions in terms of the prevention and mitigation of the landslide risk.

Landslide susceptibility assessment is one of the most debated issues nowadays; many authors have developed and performed different approaches to assess susceptibility using different parameters and algorithms, but no existing model has been implemented using input data from newspapers, chronicle notes from local and social media, unpublished catalogues, etc. Our findings show that such input data, unstructured and incomplete as they may be, are very useful to characterize areas with high tendencies for failure, and can be implemented in a user-friendly, GIS-based approach. Online networks represent a continuous source of data; using specific combinations of keyword and arguments, landslide news can be manually or automatically identified, acquired, geolocalized and organized into databases, or used to update existing ones in near-real time.

The main limitations of the resulting map of landslide prone areas is the lower level of accuracy compared to the conventional susceptibility map and the incomplete information about instability processes (number, size, type, state of activity, volume, etc.). Conversely, compared to landslides classified and used to assess conventional susceptibility maps in land-planning, it includes updated information about the occurrence of slope failures and allows continuous feedback from the real world to be incorporated. The inventory of ground effects induced by rainfall events expressly created for this study on the Entella River basin must be considered dynamic system; it will need to be updated every time a rainy event which is able to trigger shallow landslides occurs.

In light of climate change, as evidenced by the increased frequency of extreme events, the assessments made for the period examined could be subjected to slight but significant variations that will inevitably affect the vulnerability and the risk levels of the territory.

Author Contributions: The authors have very similar skills: they almost equally divided the workload. A.R. has particularly taken care of data collection, cartography and discussion of data; A.R. and A.C. have dealt with the processing of the same data (procedure on GIS to get raster map of the landslide susceptibility and then the validation starting from vector shapes); F.F., L.T. and F.L. acted as supervisors of the work in every part. L.T. and F.L. financed the research.

Funding: This research received no external funding.

Conflicts of Interest: The authors declare no conflict of interest.

References

1. Guzzetti, F. Landslide fatalities and the evaluation of landslide risk in Italy. *Eng. Geol.* **2000**, *58*, 89–107. [CrossRef]
2. Heersink, P. World Atlas of natural hazards. *Cartographica* **2005**, *40*, 133–134. [CrossRef]
3. Luino, F. Sequence of instability processes triggered by heavy rainfall in the northern Italy. *Geomorphology* **2005**, *66*, 13–39. [CrossRef]
4. Lee, M.L.; Ng, K.Y.; Huang, Y.F.; Li, W.C. Rainfall-induced landslides in Hulu Kelang area, Malaysia. *Nat. Hazards* **2014**, *70*, 353–375. [CrossRef]
5. Li, W.; Liu, C.; Hong, Y.; Sahaia, M.; Sun, W.; Yao, D.; Chen, W. Rainstorm-induced shallow landslides process and evaluation—A case study form three hot spots, China. *Geomat. Nat. Hazards Risk* **2016**, *7*, 1908–1918. [CrossRef]
6. Ban, N.; Schmidli, J.; Schär, C. Heavy precipitation in a changing climate. Does short-term summer precipitation increase faster? *Geophys. Res. Lett.* **2015**, *42*. [CrossRef]
7. European Environment Agency. *Climate Change Adaptation and Disaster Risk Reduction in Europe*; Office of the European Union: Luxembourg, 2017; Volume 15, pp. 1–171, ISSN 1725-9177.
8. Zêzere, J.L.; De Brum Ferreira, A.; Rodrigues, M.L. The role of conditioning and triggering factors in the occurrence of landslides: A case study in the area north of Lisbon (Portugal). *Geomorphology* **1999**, *30*, 133–146. [CrossRef]
9. Begueria, S. Changes in land cover and shallow landslide activity: A case study in the Spanish Pyrenees. *Geomorphology* **2006**, *74*, 196–206. [CrossRef]
10. García-Ruiz, J.M.; Lana-Renault, N. Hydrological and erosive consequences of farmland abandonment in Europe, with special reference to the Mediterranean region A review. *Agric. Ecosyst. Environ.* **2011**, *140*, 317–338. [CrossRef]

11. Ciervo, F.; Rianna, G.; Mercogliano, P.; Papa, M.N. Effects of climate change on shallow landslides in a small coastal catchment in southern Italy. *Landslides* **2017**, *14*, 1043–1055. [CrossRef]
12. Gariano, S.L.; Petrucci, O.; Guzzetti, F. The role of rainfall and land use/cover changes in landslide occurrence in Calabria, Southern Italy, in the 20th Century. In *Advancing Culture of Living with Landslides. WLF 2017*; Mikoš, M., Vilímek, V., Yin, Y., Sassa, K., Eds.; Springer: Cham, Switzerland, 2017; pp. 339–345.
13. Rago, V.; Chiaravalloti, F.; Chiodo, G.; Gabriele, S.; Lupiano, V.; Nicastro, R.; Pellegrino, A.D.; Procopio, A.; Siviglia, S.; Terranova, O.G.; et al. Geomorphic effects caused by heavy rainfall in southern Calabria (Italy) on 30 october–1 November 2015. *J. Maps* **2017**, *13*, 836–843. [CrossRef]
14. Iverson, R.M. The physics of debris flows. *Rev. Geophys.* **1997**, *35*, 245–296. [CrossRef]
15. Tropeano, D.; Turconi, L. Geomorphic classification of alpine catchments for debris-flow hazard reduction. In Proceedings of the Symposium "Debris-Flow Hazards Mitigation: Mechanics, Prediction and Assessment", Davos, Switzerland, 10–12 September 2003; Chen, R., Ed.; pp. 1221–1232.
16. Hungr, O.; Evans, S.G.; Bovis, M.J.; Hutchinson, J.N. A review of the classification of landslides of the flow type. *Environ. Eng. Geosci.* **2001**, *7*, 221–238. [CrossRef]
17. Hungr, O.; Leroueil, S.; Piccarelli, L. The Varnes classification of landslides types, an update. *Landslides* **2014**, *11*, 167–194. [CrossRef]
18. Montrasio, L.; Valentino, R. Experimental analysis and modelling of shallow landslides. *Landslides* **2007**, *4*, 291–296. [CrossRef]
19. Montgomery, D.R.; Dietrich, W.E. A physically based model for the topographic control on shallow landsliding. *Water Resour. Res.* **1994**, *30*, 1153–1171. [CrossRef]
20. Iverson, R.M. Landslide triggering by rain infiltration. *Water Resour. Res.* **2000**, *36*, 1897–1910. [CrossRef]
21. Borga, M.; Dalla Fontana, G.; Gregoretti, C.; Marchi, L. Assessment of shallow landsliding by using a physically based model of hillslope stability. *Hydrol. Process.* **2002**, *16*, 2833–2851. [CrossRef]
22. Crosta, G.B.; ì Frattini, P. Distributed modelling of shallow landslides triggered by intense rainfall. *Nat. Hazards Earth Syst. Sci.* **2003**, *3*, 81–93. [CrossRef]
23. Beek, L.P.H.V.; Asch, T.W.J.V. Regional assessment of the effects of land-use change on landslide hazard by means of physically based modelling. *Nat. Hazards* **2004**, *31*, 289–304. [CrossRef]
24. Ho, J.Y.; Lee, K.T. Performance evaluation of a physically based model for shallow landslide prediction. *Landslides* **2016**, *14*, 961–980. [CrossRef]
25. Fell, R.; Corominas, J.; Bonnard, C.; Cascini, L.; Leroi, E.; Savage, W.Z.; (on behalf of the JTC-1 Joint Technical Committee on Landslides and Engineered Slopes). Guidelines for landslide susceptibility, hazard and risk zoning for land-use planning. *Eng. Geol.* **2008**, *102*, 85–98. [CrossRef]
26. Aleotti, P.; Chowdhury, R. Landslide hazard assessment: Summary review and new perspectives. *Bull. Eng. Geol. Environ.* **1999**, *58*, 21–44. [CrossRef]
27. Guzzetti, F.; Carrara, A.; Cardinali, M.; Reichenbach, P. Landslides hazard evaluation: A review of current techniques and their application in a multi-scale study, central Italy. *Geomorphology* **1999**, *31*, 181–216. [CrossRef]
28. Reichenbach, P.; Rossi, M.; Malamud, B.D.; Mihir, M.; Guzzetti, F. A review of statistically-based landslides susceptibility models. *Earth Sci. Rev.* **2018**, *180*, 60–91. [CrossRef]
29. Van Westen, C.J.; Castellanos, E.; Kuriakose, S.L. Spatial data for landslide susceptibility, hazard, and vulnerability assessment: An overview. *Eng. Geol.* **2008**, *102*, 112–131. [CrossRef]
30. Corominas, J.; Van Westen, C.; Frattini, P.; Cascini, L.; Malet, J.P.; Fotopoulou, S.; Catani, F.; Van Den Eackhaut, M.; Mavrouli, O.; Agliardi, F.; et al. Recommendations for the quantitative analysis of landslide risk. *Bull. Eng. Geol. Environ.* **2014**, *73*, 209. [CrossRef]
31. Palladino, M.R.; Viero, A.; Turconi, L.; Brunetti, M.T.; Peruccacci, S.; Melillo, M.; Luino, F.; Deganutti, A.M.; Guzzetti, F. Rainfall thresholds for the activation of shallow landslides in the Italian Alps: The role of environmental conditioning factors. *Geomorphology* **2017**, *303*, 53–67. [CrossRef]
32. Carrara, A.; Cardinali, M.; Detti, R.; Guzzetti, F.; Pasqui, V.; Reichenbach, P. GIS techniques and statistical models in evaluating landslide hazard. *Earth Surf. Process. Landf.* **1991**, *16*, 427–445. [CrossRef]
33. Dai, F.C.; Lee, C.F. Landslide characteristics and slope instability modeling using GIS, Lantau Island, Honk Kong. *Geomorphology* **2002**, *42*, 213–228. [CrossRef]
34. Huabin, W.; Gangjun, L.; Gonghui, W. GIS-based landslides hazard assessment: An overview. *Prog. Phys. Geogr.* **2005**, *29*, 548–567. [CrossRef]

35. Cachon, J.; Irigaray, C.; Fernandez, T.; El Hamdouni, R. Engineering geology maps: Landslides and geographical information systems. *Bull. Eng. Geol. Environ.* **2006**, *65*, 341–411. [CrossRef]
36. Baeza, C.; Corominas, J. Assessment of shallow landslide susceptibility by means of multivariate statistical techniques. *Earth Surf. Process. Landf.* **2001**, *26*, 1251–1263. [CrossRef]
37. Chen, Z.; Wang, J. Landslide hazard mapping using logistic regression model in Mackenzie Valley, Canada. *Nat. Hazards* **2007**, *42*, 75–89. [CrossRef]
38. Zêzere, J.L.; Pereira, S.; Melo, R.; Oliveira, S.C.; Garcia, R.A.C. Mapping landslides susceptibility using data-driven methods. *Sci. Total Environ.* **2017**, *589*, 250–267. [CrossRef]
39. Long, N.T.; De Smedt, F. Analysis and mapping of rainfall-induced landslide susceptibility in a Luoi District, Thua Thien Hue Province, Vietnam. *Water* **2018**, *11*, 51. [CrossRef]
40. Chan, H.-C.; Chen, P.A.; Lee, J.-T. Rainfall-induced landslide susceptibility using a rainfall-runoff model and logistic regression. *Water* **2018**, *10*, 1354. [CrossRef]
41. Goetz, J.N.; Brenning, A.; Petschko, H.; Leopold, P. Evaluating machine learning and statistical prediction techniques for landslide susceptibility modelling. *Comput. Geosci.* **2015**, *81*, 1–11. [CrossRef]
42. Catani, F.; Lagomarsino, D.; Segoni, S.; Tofani, V. Landslide susceptibility estimation by random forests technique: Sensitivity and scaling issue. *Nat. Hazard Earth Syst. Sci.* **2013**, *13*, 2815–2831. [CrossRef]
43. Youssef, A.M.; Pourghasemi, H.R.; Pourtaghi, Z.S.; Al-Katheeri, M.M. Landslide susceptibility mapping using random forest, boosted regression tree, classification and regression tree, and general linear models and comparison of their performance at Wadi Tayyah Basin, Asir Region, Saudi Arabia. *Landslides* **2016**, *13*, 839–856. [CrossRef]
44. Wang, P.; Bai, X.; Wu, X.; Yu, H.; Hao, Y.; Hu, B.X. GIS-based random forest weight for rainfall-induced landslide susceptibility assessment at a humid region in Southern China. *Water* **2018**, *10*, 1019. [CrossRef]
45. Lee, S.; Ryu, J.H.; Kim, L.S. Landslide susceptibility analysis and its verification using likelihood ratio, logistic regression, and artificial neural network models: Case study of Youngin, Korea. *Landslides* **2007**, *4*, 327–338. [CrossRef]
46. Pradhan, B.; Lee, S.; Buchroithner, M.F. A GIS-based back-propagation neural network model and its cross-application and validation for landslide susceptibility analysis. *Comput. Environ. Urban Syst.* **2010**, *34*, 216–235. [CrossRef]
47. Pham, B.T.; Pradhan, B.; Bui, D.T.; Prakash, I.; Dholakia, M.B. A comparative study of different machine learning methods for landslide susceptibility assessment: A case study of Uttarakhand area (India). *Environ. Model. Soft.* **2016**, *84*, 240–250. [CrossRef]
48. Simoni, S.; Zanotti, F.; Bertoldi, G.; Rigon, R. Modelling the probability of occurrence of shallow landslides and channelized debris-flows using GEOtop-FS. *Hydrol. Process.* **2008**, *22*, 532–545. [CrossRef]
49. Anagnostopoulos, G.G.; Fatichi, S.; Burlando, P. An advanced process-based distributed model for the investigation of rainfall induced landslides: The effect of process representation and boundary conditions. *Water Resour. Res.* **2015**, *51*, 7501–7523. [CrossRef]
50. Guzzetti, F.; Stark, C.P.; Salvati, P. Evaluation of flood and landslide risk to the population of Italy. *Environ. Manag.* **2005**, *36*, 15–36. [CrossRef]
51. Faccini, F.; Robbiano, A.; Sacchini, A. Geomorphic hazard and intense rainfall: The case study of the Recco Stream Catchment (Eastern Liguria, Italy). *Nat. Hazard Earth Sys. Sci.* **2012**, *12*, 893–903. [CrossRef]
52. Faccini, F.; Luino, F.; Sacchini, A.; Turconi, L.; De Graff, J.V. Geohydrological hazards and urban development in the Mediterranean area: An example from Genoa (Liguria, Italy). *Nat. Hazards Earth Syst. Sci.* **2015**, *15*, 2631–2652. [CrossRef]
53. Giannecchini, R.; Damilano, D.; Puccinelli, A. Critical rainfall thresholds for triggering rapid shallow landslides in the Eastern Ligurian Riviera (Italy). In Proceedings of the 85th Italian Geological Society National Congress, Pisa, Italy, 6–8 September 2010; Volume 2, pp. 596–597.
54. Giannecchini, R.; Galanti, Y.; Barsanti, M. Rainfall intensity-duration thresholds for triggering shallow landslides in the Eastern Ligurian Riviera (Italy). In *Engineering Geology for Society and Territory*; Lollino, G., Giordan, D., Crosta, G.B., Corominas, J., Azzam, R., Wasowski, J., Sciarra, N., Eds.; Springer International Publishing: Basel, Switzerland, 2015; Volume 2, pp. 1581–1584.
55. Cevasco, A.; Diodato, N.; Revellino, P.; Fiorillo, F.; Grelle, G.; Guadagno, F.M. Storminess and geo-hydrological events affecting small coastal basins in a terraced Mediterranean environment. *Sci. Total Environ.* **2015**, *532*, 208–219. [CrossRef] [PubMed]

56. Cevasco, A.; Pepe, G.; D'Amato Avanzi, G.; Giannecchini, R. A study on the 10 November 2014 intense rainfall and the related landslides in the lower Lavagna valley (eastern Liguria). *Rend. Online Soc. Geol. Ital.* **2015**, *35*, 66–69. [CrossRef]
57. Cevasco, A.; Pepe, G.; D'Amato Avanzi, G.; Giannecchini, R. Preliminary analysis of the November 10, 2014 rainstorm and related landslides in the lower Lavagna Valley (Eastern Liguria). *Ital. J. Eng. Geol. Environ. Spec. Issue* **2017**, *1*, 5–15. [CrossRef]
58. D'Amato Avanzi, G.; Galanti, Y.; Giannecchini, R.; Bartelletti, C. Shallow landslides triggered by the 25 October 2011 extreme rainfall in Eastern Liguria (Italy). In *Engineering Geology for Society and Territory*; Lollino, G., Giordan, D., Crosta, G.B., Corominas, J., Azzam, R., Wasowski, J., Sciarra, N., Eds.; Springer International Publishing: Basel, Switzerland, 2015; Volume 2, pp. 515–519.
59. Cevasco, A.; Brandolini, P.; Scopesi, C.; Rellini, I. Relationships between geo-hydrological processes induced by heavy rainfall and land-use: The case of 25 October 2011 in the Vernazza catchment (Cinque Terre, NW Italy). *J. Maps* **2013**, *9*, 289–298. [CrossRef]
60. Cevasco, A.; Pepe, G.; Brandolini, P. The influences of geological and land-use settings on shallow landslides triggered by an intense rainfall event in a coastal terraced environment. *Bull. Eng. Geol. Environ.* **2014**, *73*, 859–875. [CrossRef]
61. Faccini, F.; Paliaga, G.; Piana, P.; Sacchini, A.; Watkins, C. The Bisagno stream catchment (Genoa, Italy) and its major floods: Geomorphic and land use variations in the last three centuries. *Geomorphology* **2016**, *273*, 14–27. [CrossRef]
62. Brandolini, P.; Cevasco, A.; Capolongo, D.; Pepe, G.; Lovergine, F.; Del Monte, M. Response of terraced slopes to a very intense rainfall Event and relationships with land abandonment: A case study from Cinque Terre (Italy). *Land Degrad. Dev.* **2016**, *29*, 630–642. [CrossRef]
63. Roccati, A.; Faccini, F.; Luino, F.; Turconi, L.; Piana, P.; Watkins, C.; Faccini, F. Historical geomorphological research of a Ligurian coastal floodplain (Italy) and its value for management of flood risk and environmental sustainability. *Sustainability* **2018**, *10*, 3727. [CrossRef]
64. Faccini, F.; Brandolini, P.; Robbiano, A.; Perasso, L.; Sola, A. Fenomeni di dissesto e precipitazioni in rapporto alla pianificazione territoriale: l'evento alluvionale del novembre 2002 nella bassa Val Lavagna (Liguria Orientale). *Geogr. Fis. Dinam. Quat.* **2005**, *7*, 145–153. (In Italian)
65. Faccini, F.; Piana, P.; Sacchini, A.; Lazzeri, R.; Paliaga, G.; Luino, F. Assessment of heavy rainfall triggered flash floods and landslides in the Sturla stream basin (Ligurian Apennines, northwestern Italy). *Jokull* **2017**, *67*, 44–74.
66. Roccati, A.; Faccini, F.; Luino, F.; Turconi, L.; Guzzetti, F. Rainfall events with shallow landslides in the Entella catchment, Liguria, Northern Italy. *Nat. Hazards Earth Syst. Sci.* **2018**, *18*, 2367–2386. [CrossRef]
67. Battistini, A.; Segoni, S.; Manzo, G.; Catani, F. Web data mining for automatic inventory of geohazards at national scale. *Appl. Geomorphol.* **2013**, *43*, 147–158. [CrossRef]
68. Servizio Geologico d'Italia. *Carta Geologica d'Italia in Scala 1:100,000—Foglio 83 "Rapallo"*, 2nd ed.; Servizio Geologico Italiano: Roma, Italy, 1968. (In Italian)
69. Boni, A.; Braga, G.; Conti, S.; Gelati, R.; Marchetti, G.; Passeri, L.D. *Note illustrative della Carta Geologiche d'Italia 1:100,000, Foglio 83 "Rapallo"*; Servizio Geologico Italiano: Roma, Italy, 1969. (In Italian)
70. Marini, M. L'Unità del M. Gottero fra la Val Trebbia e Sestri Levante (Appennino ligure): Nuovi dati di analisi di bacino e ipotesi di evoluzione sedimentaria. *Boll. Soc. Geol. Ital.* **1992**, *111*, 3–23. (In Italian)
71. Marini, M. Le Arenarie del M. Gottero nella sezione del M. Ramaceto (Unità del M. Gottero, Appennino ligure). *Boll. Soc. Geol. Ital.* **1994**, *113*, 283–302. (In Italian)
72. Sacchini, A.; Ferraris, F.; Faccini, F.; Firpo, M. Environmental climatic maps of Liguria. *J. Maps* **2012**, *8*, 199–207. [CrossRef]
73. Brunetti, M.T.; Peruccacci, S.; Rossi, M.; Luciani, S.; Valigi, D.; Guzzetti, F. Rainfall thresholds for the possible occurrence of landslides in Italy. *Nat. Hazards Earth Syst. Sci.* **2010**, *10*, 447–458. [CrossRef]
74. Lagomarsino, D.; Segoni, S.; Fanti, R.; Catani, F. Updating and tuning a regional-scale landslides early warning system. *Landslides* **2013**, *10*, 91–97. [CrossRef]
75. Del Ventisette, C.; Garfagnoli, F.; Ciampalini, A.; Battistini, A.; Gigli, G.; Moretti, S.; Casagli, N. An integrated approach to the study of catastrophic debris-flows: Geological hazard and human influence. *Nat. Hazards Earth Syst. Sci.* **2012**, *12*, 2907–2922. [CrossRef]

76. Santos, J.G. GIS-based hazard and risk maps of the Douro river basin (north-eastern Portugal). *Geomat. Nat. Hazard Risk* **2015**, *6*, 90–114. [CrossRef]
77. Persichillo, M.G.; Bordoni, M.; Meisina, C.; Bartelletti, C.; Barsanti, M.; Giannecchini, R.; D'Amato Avanzi, G.; Galanti, Y.; Cevasco, A.; Brandolini, P.; et al. Shallow landslides susceptibility assessment in different environments. *Geom. Nat. Hazard Risk* **2017**, *8*, 748–771. [CrossRef]
78. Pellicani, R.; Argentiero, I.; Spilotro, G. GIS-based predictive models for regional-scale landslides susceptibility assessment and risk mapping along road corridors. *Geom. Nat. Hazard Risk* **2017**, *8*, 1012–1033. [CrossRef]
79. Mathew, J.; Jha, V.K.; Rawat, G.S. Landslide susceptibility zonation mapping and its validation in part of Garhwal Lesser Himalaya, India, using a binary logistic regression analysis and receiver operating characteristic curve method. *Landslide* **2009**, *6*, 17–26. [CrossRef]
80. European Environmental Agency. *CORINE Land Cover Technical Guide. Part2 Nomenclature*; Office for Official Publications of the European Communities: Luxembourg, 1995.
81. Crosta, G.B.; Dal Negro, P.; Frattini, P. Soil slips and debris flows on terraced slopes. *Nat. Hazards Earth Syst. Sci.* **2003**, *3*, 31–42. [CrossRef]
82. Hong, H.; Naghibi, S.A.; Pourghasemi, H.R.; Pradhan, B. GIS-based landslide spatial modeling in Ganzhou City, China. *Arab. J. Geosci.* **2016**, *9*, 112. [CrossRef]
83. Bartelletti, C.; Giannecchini, R.; D'Amato Avanzi, G.; Galanti, Y.; Mazzali, A. The influence of geological-morphological and land use settings on shallow landslides in the Pogliaschina T. basin (northern Apennines, Italy). *J. Maps* **2017**, *13*, 142–152. [CrossRef]
84. Giordan, D.; Cignetti, M.; Baldo, M.; Godone, D. Relationship between man-made environment and slope stability: The case of 2014 rainfall events in the terraced landscape of the Liguria region (northwestern Italy). *Geom. Nat. Hazards Risk* **2017**, *8*, 1833–1852. [CrossRef]
85. Paliaga, G.; Faccini, F.; Luino, F.; Turconi, L.; Bobrowsky, P. Geomorphic processes and risk related to a large landslide dam in a highly urbanized Mediterranean catchment (Genoa, Italy). *Geomorphology* **2018**, *327*, 8–61. [CrossRef]